Research Paper
Computational Methods for Differential Equations
http://cmde.tabrizu.ac.ir
Vol. *, No. *, *, pp. 1-20
DOI:10.22034/cmde.2025.68655.3338

A numerical scheme with high accuracy to solve the two-dimensional time-space diffusion-wave model in terms of the Riemann-Liouville and Riesz fractional derivatives

Safar Irandoust-pakchin[1,*], MohammadHossein Derakhshan[1], and Mohamed Adel[2,*]
[1]Department of Applied Mathematics, Faculty of Mathematics, Statistics and Computer Sciences, University of Tabriz, Tabriz, Iran.
[2]Department of Mathematics, Faculty of Science, Islamic University of Madinah, Medina, KSA.

Abstract

This paper introduced a fully discrete numerical scheme for solving two-dimensional fractional diffusion equations. The time fractional derivative in the Caputo sense was discretized using a local quadratic polynomial approximation, enhancing accuracy in temporal integration. For spatial fractional derivatives of Riesz type, a nonuniform fractional central difference scheme is developed to effectively handle two-dimensional domains with variable mesh sizes. Stability and convergence analyses confirmed the robustness and precision of the method. Numerical experiments demonstrated that the scheme achieved high-order accuracy in both time and space, validated by exact solutions. The method efficiently managed nonlinear diffusion and reaction terms, showing excellent agreement between numerical and analytical results. Computational performance was evaluated through error norms and CPU time metrics, confirming the method's practicality for complex fractional models. This approach offered a flexible and accurate tool for modeling anomalous diffusion processes across various scientific and engineering applications.

Keywords. Nonuniform fractional central difference, Stability analysis, Riesz fractional derivative, Local quadratic polynomial.
2010 Mathematics Subject Classification. 26A33; 65M15; 35K57; 65M06.

1. Introduction

In recent years, fractional partial differential equations (FPDEs) have attracted growing interest from researchers in mathematics, physics, and engineering due to their ability to capture a wide range of complex phenomena [1, 6, 7, 9, 12, 13, 16, 18–20, 27, 34, 37]. These equations extend traditional integer-order models by incorporating fractional derivatives, which provide a more accurate description of processes exhibiting memory effects and anomalous transport behaviors. One of the key advantages of FPDEs is their flexibility in modeling systems with nonlocal temporal and spatial characteristics that cannot be explained by classical models. In particular, two-dimensional nonlinear time-space fractional equations have become valuable tools for investigating problems where both time-dependent memory and spatial long-range interactions influence system dynamics [2, 5, 8, 10, 17, 21–25, 30, 31, 35, 36, 40]. Such models have found applications in diverse fields, including porous media flow, groundwater contamination, viscoelastic material deformation, and biological pattern formation. The presence of nonlinearity in these models allows for the simulation of realistic physical processes with variable diffusion rates and nonlinear reaction mechanisms. Furthermore, the coupling of a time-fractional derivative, often in the Caputo sense, with a space-fractional derivative like the Riesz operator, enhances the model's capability to represent both temporal and spatial complexities simultaneously. As a result, these two-dimensional nonlinear fractional models have emerged as essential tools for understanding and predicting the behavior of many real-world systems. Developing efficient numerical schemes for solving such models remains an active and challenging area of research.

A prominent and widely applicable example of fractional modeling is the two-dimensional nonlinear diffusion-reaction system that integrates a Caputo time-fractional derivative with a Riesz space-fractional operator. This

Received: 14 August 2025 ; Accepted: 06 October 2025.
∗ Corresponding authors. Emails: s.irandoust@tabrizu.ac.ir, adel@sci.cu.edu.eg.

advanced model is particularly effective for capturing complex dynamics that are strongly influenced by both temporal memory effects and spatial nonlocal interactions. Its significance becomes evident in various real-world scenarios where classical integer-order models are insufficient. For instance, in contaminant transport within porous geological formations, this model offers a more realistic representation of pollutant spreading over time and space. Additionally, in nonlinear groundwater flow simulations, it helps to describe slow, anomalous fluid movements affected by heterogeneous subsurface structures. In the field of thermal science, the model is applicable for studying heat conduction in materials with fractal geometries, where conventional models fail to predict thermal behavior accurately. Furthermore, in biological systems, it plays a vital role in understanding pattern formation processes, such as population dynamics and tissue growth. The incorporation of nonlinear reaction terms further increases the model's ability to simulate complex chemical and biological reactions under nonlocal and history-dependent conditions. Because of its versatility and precision, this model is now considered a critical tool in both natural sciences and industrial applications, including environmental engineering, material science, and biological modeling.

The general form of the considered model can be written as:

$$\frac{\partial^\alpha u(x,y,t)}{\partial t^\alpha} = \kappa_x \frac{\partial^\beta}{\partial |x|^\beta}\left(D_x(u(x,y,t))\right) + \kappa_y \frac{\partial^\beta}{\partial |y|^\beta}\left(D_y(u(x,y,t))\right) + R(u(x,y,t)), \tag{1.1}$$

in which $0 < \alpha \leq 1$ indicates the order of the Caputo fractional derivative in time, which reflects memory effects inherent in the evolution of the process, $1 < \beta \leq 2$ corresponds to the order of the Riesz space-fractional derivative, accounting for nonlocal interactions across spatial domains, κ_x and κ_y are strictly positive constants representing diffusion intensities along the x- and y-directions, respectively, $D_x(u)$ and $D_y(u)$ denote nonlinear diffusion terms, each being a function of the unknown $u(x,y,t)$, and $R(u)$ expresses a nonlinear reaction term that may incorporate source, sink, or reactive phenomena such as chemical transformations. The Caputo time-fractional derivative of order α for a function $u(x,y,t)$ is defined as [6]:

$${}^C D_t^\alpha u(x,y,t) = \frac{1}{\Gamma(1-\alpha)} \int_0^t \frac{\partial u(x,y,\tau)/\partial \tau}{(t-\tau)^\alpha}\, d\tau, \tag{1.2}$$

where $0 < \alpha \leq 1$, $\Gamma(\cdot)$ is the Gamma function, and $\frac{\partial u}{\partial \tau}$ is the first-order partial derivative with respect to τ. The two-dimensional Riesz fractional derivative of order β, with $1 < \beta \leq 2$, acts independently on each spatial variable as follows [15]:

$$\frac{\partial^\beta u(x,y,t)}{\partial |x|^\beta} = -\frac{1}{2\cos\left(\frac{\pi\beta}{2}\right)}\left({}_{-\infty}D_x^\beta u(x,y,t) + {}_xD_\infty^\beta u(x,y,t)\right), \tag{1.3}$$

$$\frac{\partial^\beta u(x,y,t)}{\partial |y|^\beta} = -\frac{1}{2\cos\left(\frac{\pi\beta}{2}\right)}\left({}_{-\infty}D_y^\beta u(x,y,t) + {}_yD_\infty^\beta u(x,y,t)\right). \tag{1.4}$$

Here, the left- and right-sided Riemann–Liouville fractional derivatives are formulated according to [4]:

$${}_{-\infty}D_x^\beta u(x,y,t) = \frac{1}{\Gamma(m-\beta)} \frac{\partial^m}{\partial x^m} \int_{-\infty}^x \frac{u(\xi,y,t)}{(x-\xi)^{\beta-m+1}}\, d\xi,$$

$${}_xD_\infty^\beta u(x,y,t) = \frac{(-1)^m}{\Gamma(m-\beta)} \frac{\partial^m}{\partial x^m} \int_x^\infty \frac{u(\xi,y,t)}{(\xi-x)^{\beta-m+1}}\, d\xi,$$

and similarly for the y-direction,

$${}_{-\infty}D_y^\beta u(x,y,t) = \frac{1}{\Gamma(m-\beta)} \frac{\partial^m}{\partial y^m} \int_{-\infty}^y \frac{u(x,\eta,t)}{(y-\eta)^{\beta-m+1}}\, d\eta,$$

$${}_yD_\infty^\beta u(x,y,t) = \frac{(-1)^m}{\Gamma(m-\beta)} \frac{\partial^m}{\partial y^m} \int_y^\infty \frac{u(x,\eta,t)}{(\eta-y)^{\beta-m+1}}\, d\eta,$$

where $m = \lceil \beta \rceil$.

This nonlinear fractional model offers a sophisticated mathematical framework designed to describe transport and reaction phenomena in complex media where both long-range spatial dependencies and memory effects in time play crucial roles. By integrating fractional derivatives in both space and time, the model captures the intricate interplay between spatial nonlocality and temporal history that is often observed in heterogeneous and fractal-like materials. The nonlinear terms in the diffusion and reaction components allow the model to effectively simulate a wide range of real-world processes characterized by nonlinear interactions and feedback mechanisms. Such processes include the spread of pollutants in porous soils, where contaminant transport deviates from classical diffusion due to complex pore structures. In ecological and biological systems, the model is valuable for analyzing population dynamics with memory effects, such as species dispersal influenced by past environmental conditions. Furthermore, it has been successfully applied to thermal transport in materials with irregular microstructures, capturing anomalous heat flow that traditional integer-order models cannot describe accurately. This comprehensive approach makes the model highly relevant not only in environmental science and biology but also in industrial applications involving materials engineering and chemical reactions. The ability to incorporate both spatial and temporal fractional derivatives along with nonlinearity provides a powerful tool for researchers to predict and control complex dynamical systems in various scientific and engineering fields.

The combined influence of nonlinearity, memory effects, and spatial nonlocality significantly increases the complexity of the fractional model. These factors make it difficult to derive exact analytical solutions, as classical methods often fall short in handling such intricacies. Consequently, the design and implementation of stable, efficient, and accurate numerical algorithms become essential for effectively solving these equations. Developing such robust numerical schemes remains a vibrant and challenging research area, attracting considerable attention from scientists and engineers alike. In this study, a comprehensive discrete numerical framework was proposed for addressing two-dimensional fractional diffusion equations. The temporal fractional derivative, defined in the Caputo sense, was approximated using a locally adapted quadratic interpolation, significantly improving the temporal resolution and accuracy of the solution. To discretize the Riesz-type spatial fractional derivatives, a nonuniform fractional centered difference technique was designed, enabling precise modeling over irregular two-dimensional spatial grids with varying step sizes. Rigorous stability and convergence evaluations confirmed the method's reliability and computational robustness. Extensive numerical tests, benchmarked against known analytical solutions, verified that the scheme delivers high-order accuracy in both spatial and temporal dimensions. The approach demonstrated particular effectiveness in tackling nonlinear diffusion-reaction systems, showing a strong correlation between simulated and exact results. Furthermore, by assessing error metrics and CPU runtime performance, the algorithm's efficiency and suitability for large-scale and complex fractional diffusion models were established. This makes the method a versatile and accurate computational tool for simulating anomalous diffusion phenomena encountered in diverse scientific and engineering fields.

Numerical techniques serve as indispensable tools for addressing mathematical models that lack exact analytical solutions. This is particularly true for real-world systems characterized by intricate geometries, nonlinear behavior, or fractional calculus, where obtaining closed-form solutions is either highly impractical or impossible. These computational approaches provide versatile and efficient means to approximate solutions with controllable accuracy, thereby allowing researchers to explore and study models that would otherwise be analytically inaccessible. With the continuous advancement of computational resources, numerical algorithms have become especially viable for solving complex problems across scientific and engineering disciplines. In [32], Shams and collaborators introduced a modified single-step fractional iterative algorithm based on a one-parameter Caputo-type family. Their convergence analysis established the convergence order of the method, and the symbolic software CAS-Maple was employed to derive the associated error expressions. The robustness and effectiveness of their approach were validated through several applications in civil and chemical engineering, where the new method demonstrated superior performance in terms of error reduction, computational efficiency, and convergence rate compared to conventional fractional schemes. Derakhshan et al. in [11] presented a hybrid numerical method tailored for the time-space fractional diffusion model incorporating Caputo and Riesz derivatives. This approach combines quadratic and linear interpolation techniques to approximate the time-fractional derivative and achieves both high precision and low computational overhead. Theoretical investigations confirmed the stability and convergence of the proposed algorithm. In a separate study, Shi et al. [33] explored neural network-based strategies for solving fractional differential equations. They developed a physics-informed neural network (fPINN) framework tailored to the time-fractional Huxley equation. This method embeds the underlying physical laws within the training process, enabling the network to approximate solutions with high fidelity. Lu and colleagues [26] examined the robust asymptotic stability of fractional-order linear systems under structured uncertainties. Leveraging Kronecker products and μ-analysis, they transformed the problem into verifying the non-singularity of a certain class of perturbed matrices, and established both necessary and sufficient conditions for stability—extending beyond previously considered interval systems. In [28], Owolabi addressed the numerical treatment of space–time fractional reaction–diffusion systems governed by Caputo and Riesz operators, modeling anomalous transport phenomena. A flexible numerical framework was introduced to approximate these operators effectively, enabling simulation of systems with non-classical diffusion dynamics. Deng et al. [14] proposed a high-order accurate scheme for the time-fractional Gray–Scott model, which is known for exhibiting singular behavior at the initial time. By employing Euler's beta function, they investigated the regularity of the solution and applied decomposition techniques to enhance accuracy. Zhang and Ding contributed a second-order finite difference approximation for the Riesz fractional operator and utilized the Crank–Nicolson method for time discretization. Their algorithm for two-dimensional fractional diffusion equations was rigorously shown—via the energy method—to be both stable and convergent. Furthermore, by incorporating higher-order perturbations, they extended the scheme to an alternating direction implicit (ADI) method, increasing computational performance without sacrificing accuracy. In another advancement, Alqhtani et al. [3] proposed a numerical framework for solving Riesz-type fractional parabolic equations. Motivated by the role of Riesz operators in modeling anomalous diffusion and dispersion, their work extends classical Brownian motion models via space-fractional formulations, offering improved modeling fidelity in various physical systems. Qu et al. [29] designed a novel fourth-order finite difference method integrated with Crank–Nicolson explicit linearization to handle nonlinear two-dimensional Riesz fractional reaction–diffusion systems. The explicit treatment of nonlinearities, under a Lipschitz condition, allowed the authors to prove unconditional stability and enhance overall computational accuracy. Lastly, Zhang et al. [38] developed a second-order numerical approach for nonlinear Riesz space-fractional diffusion equations. The spatial derivatives were discretized using a fractional central difference scheme, while time integration was handled via the Crank–Nicolson method. To manage the nonlinearity, they employed explicit linearization, and efficiently solved the resulting ill-conditioned Toeplitz systems using the fast sine transform (FST), thereby accelerating computations and improving accuracy for large-scale problems.

The structure of this paper is organized as follows. In section 2, we focus on the discretization of the two-dimensional Caputo fractional derivative by employing a local quadratic polynomial approximation, which enhances the accuracy of temporal integration for the proposed model. Additionally, this section presents the semi-discrete time discretization of the governing equation and provides a comprehensive convergence analysis of the resulting semi-discrete numerical scheme to ensure its theoretical validity and computational reliability. In section 3, attention is directed towards the spatial discretization of the two-dimensional Riesz fractional derivatives using a nonuniform fractional central difference scheme. This approach effectively handles irregular spatial meshes and captures the complexities of fractional spatial operators. Furthermore, this section introduces the full discretization of the proposed two-dimensional nonlinear time-space fractional model, integrating both time and space discretization strategies into a unified framework. Section 4 is dedicated to the stability analysis of the fully discrete fractional scheme, where we rigorously prove the unconditional stability of the numerical method under appropriate conditions. In section 5, we conduct a detailed error analysis for the fully discrete scheme, establishing error bounds and demonstrating the scheme's convergence order both in time and space. Section 6 presents several numerical simulations and illustrative examples that validate the theoretical findings and demonstrate the accuracy, efficiency, and practical applicability of the proposed method for solving complex nonlinear fractional diffusion problems. Finally, section 7 summarizes the main conclusions drawn from this study and outlines possible directions for future research on high-order numerical methods for time-space fractional partial differential equations.

2. Discretization of the Two-Dimensional Caputo Fractional Derivative Using Local Quadratic Polynomial Approximation

In this section, we extend the detailed discretization scheme of the Caputo fractional derivative to a two-dimensional spatial domain (x, y) with respect to time t. For a sufficiently smooth function $u(x, y, t)$, the Caputo fractional derivative of order $\alpha \in (0,1)$ in time at a fixed spatial point (x_i, y_j) and time $t = t_n$ is defined by

$$ {}^C D_t^\alpha u(x_i, y_j, t_n) = \frac{1}{\Gamma(1-\alpha)} \int_0^{t_n} \frac{\partial u(x_i, y_j, \tau)/\partial \tau}{(t_n - \tau)^\alpha} \, d\tau. \tag{2.1} $$

We discretize the time interval $[0, t_n]$ into n subintervals:

$$ 0 = s_0 < s_1 < \cdots < s_{n-1} < s_n = t_n, $$

and on each subinterval $[s_{m-1}, s_m]$, approximate the time derivative $\partial u/\partial t$ at fixed (x_i, y_j) by a local quadratic polynomial:

$$ P_m^{i,j}(\tau) = a_m^{i,j}(\tau - c_m)^2 + b_m^{i,j}(\tau - c_m) + d_m^{i,j}, $$

where

$$ c_m = \frac{s_{m-1} + s_m}{2}, $$

and coefficients $a_m^{i,j}, b_m^{i,j}, d_m^{i,j}$ are determined by interpolating $\partial u/\partial t$ at $\tau = s_{m-1}, s_m, c_m$ at the spatial grid point (x_i, y_j). The Caputo derivative integral becomes a sum over the temporal subintervals:

$$ {}^C D_t^\alpha u(x_i, y_j, t_n) = \frac{1}{\Gamma(1-\alpha)} \sum_{m=1}^{n} I_m^{i,j}, \tag{2.2} $$

with

$$ I_m^{i,j} = \int_{s_{m-1}}^{s_m} \frac{\partial u(x_i, y_j, \tau)/\partial \tau}{(t_n - \tau)^\alpha} d\tau \approx \int_{s_{m-1}}^{s_m} \frac{P_m^{i,j}(\tau)}{(t_n - \tau)^\alpha} d\tau. $$

Following the same procedure as in the one-dimensional case, define:

$$ h_m = s_m - s_{m-1}, \quad \Delta_m = s_{m-1} - c_m = -\frac{h_m}{2}. $$

Change variable

$$ z = \frac{\tau - s_{m-1}}{h_m} \in [0,1], $$

and rewrite

$$ I_m^{i,j} \approx h_m \int_0^1 \frac{a_m^{i,j}(\Delta_m + h_m z)^2 + b_m^{i,j}(\Delta_m + h_m z) + d_m^{i,j}}{(t_n - s_{m-1} - h_m z)^\alpha} dz. $$

Set polynomial coefficients for each spatial point (x_i, y_j):

$$ \begin{aligned} A_m^{i,j} &= a_m^{i,j}\Delta_m^2 + b_m^{i,j}\Delta_m + d_m^{i,j}, \\ B_m^{i,j} &= 2a_m^{i,j}\Delta_m h_m + b_m^{i,j} h_m, \\ C_m^{i,j} &= a_m^{i,j} h_m^2. \end{aligned} $$

The integral becomes

$$ I_m^{i,j} \approx h_m \left(A_m^{i,j} J_0 + B_m^{i,j} J_1 + C_m^{i,j} J_2 \right), $$

where

$$ J_k = \int_0^1 \frac{z^k}{(D_m - h_m z)^\alpha} dz, \quad D_m = t_n - s_{m-1}, \quad k = 0, 1, 2. $$

As before, change variables to express J_k via the incomplete Beta function:

$$ J_k = \frac{D_m^{k+1-\alpha}}{h_m^{k+1}} B_\eta(k+1, 1-\alpha), \quad \eta = \frac{h_m}{D_m} < 1. $$

Therefore,

$$I_m^{i,j} \approx \sum_{k=0}^{2} C_{m,k}^{i,j} \frac{(t_n - s_{m-1})^{k+1-\alpha}}{(s_m - s_{m-1})^k} B_{\frac{s_m - s_{m-1}}{t_n - s_{m-1}}}(k+1, 1-\alpha), \tag{2.3}$$

with $C_{m,0}^{i,j} = A_m^{i,j}, C_{m,1}^{i,j} = B_m^{i,j}, C_{m,2}^{i,j} = C_m^{i,j}$. The full discrete approximation of the Caputo derivative at (x_i, y_j, t_n) reads

$${}^{C}D_t^{\alpha} u(x_i, y_j, t_n) \approx \frac{1}{\Gamma(1-\alpha)} \sum_{m=1}^{n} I_m^{i,j}. \tag{2.4}$$

The accuracy of the proposed discretization for the Caputo time-fractional derivative depends primarily on the interpolation error introduced by approximating the time derivative $\frac{\partial u(x_i,y_j,t)}{\partial t}$ with a local quadratic polynomial over each subinterval $[s_{m-1}, s_m]$. Let $h_m = s_m - s_{m-1}$ denote the length of the m-th time subinterval, and assume that $u(x, y, t)$ has continuous fourth-order partial derivatives with respect to time in $[0, t_n]$ for each spatial location (x_i, y_j). The local interpolation error for approximating the time derivative on each subinterval satisfies:

$$\left| \frac{\partial u(x_i, y_j, \tau)}{\partial t} - P_m^{i,j}(\tau) \right| \leq \frac{M^{i,j}}{6} h_m^3, \quad \forall \tau \in [s_{m-1}, s_m], \tag{2.5}$$

where

$$M^{i,j} = \max_{\tau \in [s_{m-1}, s_m]} \left| \frac{\partial^4 u(x_i, y_j, \tau)}{\partial t^4} \right|.$$

Considering the weakly singular kernel $(t_n - \tau)^{-\alpha}$ in the Caputo derivative integral, the total global discretization error $\varepsilon^{i,j}$ at the spatial point (x_i, y_j) and time t_n is bounded by:

$$\left|\varepsilon^{i,j}\right| \leq \frac{C^{i,j}}{\Gamma(1-\alpha)} \sum_{m=1}^{n} h_m^4 (t_n - s_{m-1})^{-\alpha}, \tag{2.6}$$

where

$$C^{i,j} = \frac{M^{i,j}}{6}.$$

For uniform time steps $h_m = h$, this reduces to:

$$\left|\varepsilon^{i,j}\right| \leq C^{i,j} \cdot \frac{h^3}{\Gamma(1-\alpha)} \sum_{m=1}^{n} (t_n - s_{m-1})^{-\alpha}. \tag{2.7}$$

For total time $t_n = n\Delta t$, this gives the following error estimate:

$$\left|\varepsilon^{i,j}\right| = O(\Delta t^3 \cdot t_n^{1-\alpha}), \tag{2.8}$$

where the error order is $O(\Delta t^3)$ due to the cubic interpolation, and the factor $t_n^{1-\alpha}$ comes from the time-fractional integral kernel.

2.1. **Semi-Discrete Time Discretization of the Proposed Model.** In this subsection, we develop a semi-discrete numerical scheme for the proposed two-dimensional nonlinear time-space fractional diffusion-reaction model which is given in Eq. (1.1), where the time-fractional derivative is discretized using a quadratic interpolation-based scheme, while the spatial operators remain in continuous form. Let the time domain $[0, T]$ be divided into N uniform intervals with time step size Δt, so that $t_n = n\Delta t$ for $n = 0, 1, 2, \ldots, N$. The Caputo fractional derivative at time t_n is approximated at each spatial point (x_i, y_j) using the quadratic interpolation-based discrete formula:

$${}^{C}D_t^{\alpha} u(x_i, y_j, t_n) \approx \frac{1}{\Gamma(1-\alpha)} \sum_{m=1}^{n} I_m^{i,j}, \tag{2.9}$$

where

$$I_m^{i,j} = A_m \left(u_{i,j}^{m-1}\right) + B_m \left(u_{i,j}^{m}\right) + C_m \left(u_{i,j}^{m+1}\right), \tag{2.10}$$

and the coefficients A_m, B_m, and C_m are derived from the analytical integration of the quadratic interpolating polynomial over $[t_{m-1}, t_m]$, as shown in section 2. By substituting the discrete approximation (2.9) into the main Equation (1.1), we obtain the following semi-discrete form at time level t_n for each grid point (x_i, y_j):

$$\frac{1}{\Gamma(1-\alpha)} \sum_{m=1}^{n} \left[A_m \left(u_{i,j}^{m-1}\right) + B_m \left(u_{i,j}^{m}\right) + C_m \left(u_{i,j}^{m+1}\right)\right] = \kappa_x \frac{\partial^\beta}{\partial |x|^\beta} \left(D_x(u_{i,j}^n)\right) + \kappa_y \frac{\partial^\beta}{\partial |y|^\beta} \left(D_y(u_{i,j}^n)\right) + R\left(u_{i,j}^n\right). \quad (2.11)$$

Here, $u_{i,j}^n$ denotes the numerical approximation of $u(x_i, y_j, t_n)$ at time level n. The local truncation error $\tau_{i,j}^n$ of the time discretization at point (x_i, y_j) and time level t_n can be estimated as:

$$\tau_{i,j}^n = C_\alpha h^3 \cdot \max_{t\in[0,t_n]} \left| \frac{d^3}{dt^3} u(x_i, y_j, t) \right|, \quad (2.12)$$

where C_α is a positive constant dependent on the fractional order α and the interpolation kernel. This shows that the proposed scheme achieves third-order accuracy in time for smooth solutions. In Table 1, a detailed step-by-step procedure for implementing the semi-discrete numerical method is presented, with an emphasis on time discretization using the Caputo fractional derivative approximation. The table demonstrates how spatial derivatives and nonlinear terms remain continuous, while the discretization is applied solely to the time derivatives. Additionally, it summarizes the expected order of accuracy and the corresponding error bounds associated with the time discretization scheme.

Algorithm 1 Semi-discrete numerical method for time-fractional derivative

1: **Time-fractional derivative approximation:** Approximate the Caputo fractional derivative in time at time level t_n using

$$\frac{\partial^\alpha u(x, y, t_n)}{\partial t^\alpha} \approx \frac{1}{\Gamma(1-\alpha)} \sum_{m=1}^{n} \left[A_m u_{i,j}^{m-1} + B_m u_{i,j}^{m} + C_m u_{i,j}^{m+1}\right]$$

where coefficients A_m, B_m, C_m depend on the discretization scheme and step size Δt.

2: **Spatial derivatives treated continuously:** Keep the Riesz fractional derivatives and nonlinear reaction terms continuous in space:

$$\kappa_x \frac{\partial^\beta}{\partial |x|^\beta} \left(D_x(u_{i,j}^n)\right) + \kappa_y \frac{\partial^\beta}{\partial |y|^\beta} \left(D_y(u_{i,j}^n)\right) + R(u_{i,j}^n)$$

3: **Semi-discrete scheme:** Combine the above approximations to get the semi-discrete equation at time t_n:

$$\frac{1}{\Gamma(1-\alpha)} \sum_{m=1}^{n} \left[A_m u_{i,j}^{m-1} + B_m u_{i,j}^{m} + C_m u_{i,j}^{m+1}\right] = \kappa_x \frac{\partial^\beta}{\partial |x|^\beta} \left(D_x(u_{i,j}^n)\right) + \kappa_y \frac{\partial^\beta}{\partial |y|^\beta} \left(D_y(u_{i,j}^n)\right) + R(u_{i,j}^n)$$

4: **Error estimation:** The truncation error in time is bounded by $\mathcal{O}(\Delta t^{2-\alpha})$, indicating convergence order dependent on fractional order α.

2.2. **Convergence Analysis of the Semi-Discrete Numerical Scheme.** In this subsection, we provide a rigorous convergence analysis for the proposed semi-discrete numerical scheme in the time direction for solving the nonlinear two-dimensional time-space fractional diffusion-reaction model. The analysis focuses on the error between the exact solution and the numerical approximation obtained by the quadratic interpolation-based time discretization.

Theorem 2.1. *Let $u(x, y, t)$ be the exact solution of the model (1.1) with sufficient smoothness, and let $u_{i,j}^n$ denote the numerical approximation obtained using the proposed semi-discrete scheme (2.11) at spatial point (x_i, y_j) and time level t_n. Assume that $u(x, y, t)$ satisfies:*

$$\left| \frac{\partial^3 u(x, y, t)}{\partial t^3} \right| \le M, \quad \forall (x, y, t) \in \Omega \times [0, T],$$

where $M > 0$ is a positive constant. Then, the numerical scheme is convergent in time, and the global discretization error $e_{i,j}^n = u(x_i, y_j, t_n) - u_{i,j}^n$ satisfies the following bound:

$$|e_{i,j}^n| \leq C \cdot \Delta t^2, \tag{2.13}$$

where Δt is the time step size and C is a constant independent of Δt, but dependent on T, α, and the third time derivative of the exact solution.

Proof. Let us define the local truncation error $\tau_{i,j}^n$ at time level t_n and spatial point (x_i, y_j) as:

$$\tau_{i,j}^n = {}^C D_t^\alpha u(x_i, y_j, t_n) - \frac{1}{\Gamma(1-\alpha)} \sum_{m=1}^{n} \left[A_m u_{i,j}^{m-1} + B_m u_{i,j}^m + C_m u_{i,j}^{m+1} \right], \tag{2.14}$$

where A_m, B_m, and C_m are the discrete coefficients defined in Section 3. Using the standard remainder formula for quadratic interpolation and properties of the Caputo derivative, it can be shown that:

$$|\tau_{i,j}^n| \leq K_\alpha \Delta t^2 \cdot \max_{t \in [0, t_n]} \left| \frac{\partial^3 u(x_i, y_j, t)}{\partial t^3} \right|, \tag{2.15}$$

where K_α is a constant depending only on the fractional order α. Next, by applying the discrete Grönwall inequality (or fractional discrete Grönwall lemma) for the error propagation equation derived from subtracting the numerical scheme from the exact equation, we obtain:

$$|e_{i,j}^n| \leq C \left(\max_{1 \leq m \leq n} |\tau_{i,j}^m| \right), \tag{2.16}$$

where C is a constant depending on the final time T, fractional order α, and the Lipschitz constant of the nonlinear terms. Finally, substituting the local error bound (2.15) into (2.16), we conclude that:

$$|e_{i,j}^n| \leq C' \cdot \Delta t^2,$$

where $C' = C \cdot K_\alpha \cdot M$, completing the proof. □

3. Spatial Discretization of Two-Dimensional Riesz Fractional Derivatives Using a Nonuniform Fractional Central Difference Scheme

In this section, we introduce a novel and less commonly used approach for the spatial discretization of the two-dimensional Riesz space-fractional derivatives appearing in the proposed model (1.1). The method is based on a nonuniform fractional central difference operator, which provides enhanced flexibility for handling spatial heterogeneities and sharp gradients in the solution. The Riesz space-fractional derivative of order $\beta \in (1, 2)$ in the x and y directions for a sufficiently smooth function $u(x, y, t)$ is defined in Eqs. (1.3) and (1.4). To discretize the above derivatives, we consider a nonuniform grid along the x and y directions. Let x_i and y_j denote the grid points with spatial step sizes $\Delta x_i = x_i - x_{i-1}$ and $\Delta y_j = y_j - y_{j-1}$, which may vary across the domain. The discrete approximation of the Riesz fractional derivative in the x-direction at grid point (x_i, y_j) and time level n is given by:

$$\frac{\partial^\beta u_{i,j}^n}{\partial |x|^\beta} \approx -c_\beta \left(\frac{1}{(\Delta x_i)^\beta} \sum_{k=1}^{i} w_k^{(\beta)} u_{i-k,j}^n + \frac{1}{(\Delta x_{i+1})^\beta} \sum_{k=1}^{M-i} w_k^{(\beta)} u_{i+k,j}^n \right), \tag{3.1}$$

where $w_k^{(\beta)}$ are the nonuniform fractional weights defined as:

$$w_k^{(\beta)} = (-1)^k \binom{\beta}{k} = \frac{(-1)^k \Gamma(\beta+1)}{\Gamma(k+1)\Gamma(\beta-k+1)}, \tag{3.2}$$

for $k \geq 1$, and M denotes the total number of spatial grid points in the x-direction. Similarly, the Riesz derivative in the y-direction is discretized as:

$$\frac{\partial^\beta u_{i,j}^n}{\partial |y|^\beta} \approx -c_\beta \left(\frac{1}{(\Delta y_j)^\beta} \sum_{k=1}^{j} w_k^{(\beta)} u_{i,j-k}^n + \frac{1}{(\Delta y_{j+1})^\beta} \sum_{k=1}^{L-j} w_k^{(\beta)} u_{i,j+k}^n \right), \tag{3.3}$$

where L is the total number of grid points in the y-direction. The local truncation error for the nonuniform fractional central difference scheme for the Riesz derivative at grid point (x_i, y_j) and time level n is expressed as:

$$LTE_{i,j}^{x} = \left| \frac{\partial^\beta u_{i,j}^n}{\partial |x|^\beta} - \Big(-c_\beta \left[\frac{1}{(\Delta x_i)^\beta} \sum_{k=1}^{i} w_k^{(\beta)} u_{i-k,j}^n + \frac{1}{(\Delta x_{i+1})^\beta} \sum_{k=1}^{M-i} w_k^{(\beta)} u_{i+k,j}^n \right] \Big) \right|, \tag{3.4}$$

$$LTE_{i,j}^{y} = \left| \frac{\partial^\beta u_{i,j}^n}{\partial |y|^\beta} - \Big(-c_\beta \left[\frac{1}{(\Delta y_j)^\beta} \sum_{k=1}^{j} w_k^{(\beta)} u_{i,j-k}^n + \frac{1}{(\Delta y_{j+1})^\beta} \sum_{k=1}^{L-j} w_k^{(\beta)} u_{i,j+k}^n \right] \Big) \right|. \tag{3.5}$$

The total local spatial discretization error at (x_i, y_j) is then:

$$LTE_{i,j}^{space} = LTE_{i,j}^{x} + LTE_{i,j}^{y}. \tag{3.6}$$

3.1. **Full Discretization of the Proposed Two-Dimensional Nonlinear Time-Space Fractional Model.** In this section, we derive the fully-discrete numerical scheme for the proposed two-dimensional nonlinear time-space fractional model given in (1.1). This is achieved by combining the time discretization based on the newly proposed weighted finite difference approximation for the Caputo fractional derivative (as presented in the semi-discrete scheme) with the nonuniform fractional central difference method for the spatial Riesz fractional derivatives.

The full-discrete form of the governing equation at grid point (x_i, y_j) and time level n is written as:

$$\begin{aligned} \frac{1}{\Gamma(1-\alpha)} \sum_{m=1}^{n} \left[A_m\, u_{i,j}^{m-1} + B_m\, u_{i,j}^{m} + C_m\, u_{i,j}^{m+1} \right] = \kappa_x &\left(-c_\beta \left[\frac{1}{(\Delta x_i)^\beta} \sum_{k=1}^{i} w_k^{(\beta)} u_{i-k,j}^n + \frac{1}{(\Delta x_{i+1})^\beta} \sum_{k=1}^{M-i} w_k^{(\beta)} u_{i+k,j}^n \right] \right) \\ &+ \kappa_y \left(-c_\beta \left[\frac{1}{(\Delta y_j)^\beta} \sum_{k=1}^{j} w_k^{(\beta)} u_{i,j-k}^n + \frac{1}{(\Delta y_{j+1})^\beta} \sum_{k=1}^{L-j} w_k^{(\beta)} u_{i,j+k}^n \right] \right) \\ &+ R(u_{i,j}^n). \end{aligned} \tag{3.7}$$

The total local truncation error (LTE) of the full-discrete scheme at grid point (x_i, y_j) and time level n consists of two main components: the temporal discretization error ($LTE_{i,j}^{time}$) and the spatial discretization error ($LTE_{i,j}^{space}$). The local truncation error due to time discretization, based on the finite difference approximation of the Caputo derivative, is given by:

$$LTE_{i,j}^{time} = C_1\, \Delta t^p + \mathcal{O}(\Delta t^p), \tag{3.8}$$

where p denotes the order of convergence in time (depending on the specific weights used), and C_1 is a constant. The spatial discretization error resulting from the nonuniform fractional central difference approximation of the Riesz derivative in both directions is given by:

$$LTE_{i,j}^{space} = C_2\left((\max \Delta x_i)^q + (\max \Delta y_j)^q \right) + \mathcal{O}\left((\max \Delta x_i)^q + (\max \Delta y_j)^q \right), \tag{3.9}$$

where q represents the spatial convergence order and C_2 is a constant. The total LTE at (x_i, y_j) and time level n is then:

$$LTE_{i,j}^{total} = LTE_{i,j}^{time} + LTE_{i,j}^{space}. \tag{3.10}$$

Table 2 summarizes the step-by-step procedure of the fully discrete numerical method for solving the proposed fractional model. It details the initialization, computation of fractional derivative weights, and iterative update of the solution at each time step. This framework ensures accurate approximation of both time-fractional Caputo and space-fractional Riesz derivatives with nonlinear reaction terms.

Algorithm 2 Fully discrete numerical method for the fractional model

1: **Initialization:** Set spatial grid points (x_i, y_j), temporal points t_n, fractional orders α, β, and coefficients κ_x, κ_y.
2: **Initial condition:** Assign $u^0_{i,j} = u_0(x_i, y_j)$ for all spatial nodes.
3: **Time-derivative weights:** Compute Caputo fractional time-derivative weights A_m, B_m, and C_m for order α.
4: **Spatial-derivative weights:** Calculate Riesz fractional spatial derivative weights $w_k^{(\beta)}$ for both x- and y-directions based on β.
5: **Time-stepping procedure:** For each time step $n = 1, 2, \ldots, N$ and spatial node (i, j):
   (1) Evaluate the fractional time derivative term
   $$\frac{1}{\Gamma(1-\alpha)} \sum_{m=1}^{n} \left(A_m u^{m-1}_{i,j} + B_m u^m_{i,j} + C_m u^{m+1}_{i,j} \right).$$
   (2) Approximate the Riesz fractional derivatives in space using discrete convolution sums with weights $w_k^{(\beta)}$.
   (3) Compute the nonlinear reaction term $R(u^n_{i,j})$.
   (4) Solve the resulting algebraic equation to obtain $u^n_{i,j}$.
6: **Boundary conditions:** Apply appropriate boundary conditions at each time level.
7: **Termination:** Repeat the above steps until the final time step, then analyze results for stability and convergence.

4. Stability Analysis of the Fully Discrete Fractional Scheme

Consider the fully discrete numerical scheme for the two-dimensional nonlinear fractional diffusion-reaction equation given by Equation (3.7). Prove stability of the scheme in the discrete l_2-norm under suitable conditions. Define the discrete l_2-norm over spatial grid points as

$$\|u^n\|^2 = \sum_{i=1}^{M} \sum_{j=1}^{L} \left(u^n_{i,j}\right)^2 \Delta x_i \Delta y_j.$$

Multiply both sides by $u^n_{i,j}$ and sum over all spatial indices:

$$\begin{aligned}
&\frac{1}{\Gamma(1-\alpha)} \sum_{i=1}^{M} \sum_{j=1}^{L} u^n_{i,j} \sum_{m=1}^{n} \left(A_m u^{m-1}_{i,j} + B_m u^m_{i,j} + C_m u^{m+1}_{i,j} \right) \Delta x_i \Delta y_j \\
&= \sum_{i=1}^{M} \sum_{j=1}^{L} u^n_{i,j} \Bigg\{ \kappa_x \left(-c_\beta \left[\frac{1}{(\Delta x_i)^\beta} \sum_{k=1}^{i} w_k^{(\beta)} u^n_{i-k,j} + \frac{1}{(\Delta x_{i+1})^\beta} \sum_{k=1}^{M-i} w_k^{(\beta)} u^n_{i+k,j} \right] \right) \\
&+ \kappa_y \left(-c_\beta \left[\frac{1}{(\Delta y_j)^\beta} \sum_{k=1}^{j} w_k^{(\beta)} u^n_{i,j-k} + \frac{1}{(\Delta y_{j+1})^\beta} \sum_{k=1}^{L-j} w_k^{(\beta)} u^n_{i,j+k} \right] \right) + R(u^n_{i,j}) \Bigg\} \Delta x_i \Delta y_j.
\end{aligned}$$

By discrete fractional calculus results, the left-hand side satisfies

$$\frac{1}{\Gamma(1-\alpha)} \sum_{i,j} u^n_{i,j} \sum_{m=1}^{n} \left(A_m u^{m-1}_{i,j} + B_m u^m_{i,j} + C_m u^{m+1}_{i,j} \right) \Delta x_i \Delta y_j \geq \frac{1}{2} D_t^\alpha \|u^n\|^2,$$

where the discrete fractional time derivative $D_t^\alpha \|u^n\|^2$ is defined by

$$D_t^\alpha \|u^n\|^2 := \frac{1}{\tau^\alpha} \sum_{m=0}^{n} g_{n-m} \left(\|u^m\|^2 - \|u^{m-1}\|^2 \right),$$

and $g_k > 0$ depend on α and discretization parameters. Using properties of fractional difference operators and symmetry,

$$\sum_{i,j} u_{i,j}^n \kappa_x \left(-c_\beta \left[\frac{1}{(\Delta x_i)^\beta} \sum_{k=1}^{i} w_k^{(\beta)} u_{i-k,j}^n + \frac{1}{(\Delta x_{i+1})^\beta} \sum_{k=1}^{M-i} w_k^{(\beta)} u_{i+k,j}^n \right] \right) \Delta x_i \Delta y_j \le -\Lambda_x \|u^n\|^2,$$

and similarly for the y-direction,

$$\sum_{i,j} u_{i,j}^n \kappa_y \left(-c_\beta \left[\frac{1}{(\Delta y_j)^\beta} \sum_{k=1}^{j} w_k^{(\beta)} u_{i,j-k}^n + \frac{1}{(\Delta y_{j+1})^\beta} \sum_{k=1}^{L-j} w_k^{(\beta)} u_{i,j+k}^n \right] \right) \Delta x_i \Delta y_j \le -\Lambda_y \|u^n\|^2,$$

where $\Lambda_x, \Lambda_y > 0$ depend on the mesh and problem parameters. Hence,

$$\sum_{i,j} u_{i,j}^n \Bigg[-c_\beta \left(\frac{1}{(\Delta x_i)^\beta} \sum_{k=1}^{i} w_k^{(\beta)} u_{i-k,j}^n + \frac{1}{(\Delta x_{i+1})^\beta} \sum_{k=1}^{M-i} w_k^{(\beta)} u_{i+k,j}^n \right)$$
$$-c_\beta \left(\frac{1}{(\Delta y_j)^\beta} \sum_{k=1}^{j} w_k^{(\beta)} u_{i,j-k}^n + \frac{1}{(\Delta y_{j+1})^\beta} \sum_{k=1}^{L-j} w_k^{(\beta)} u_{i,j+k}^n \right) \Bigg] \Delta x_i \Delta y_j \le -\Lambda \|u^n\|^2,$$

with $\Lambda = \Lambda_x + \Lambda_y > 0$. Suppose $R(\cdot)$ satisfies the Lipschitz condition

$$|R(u) - R(v)| \le L_R |u - v|,$$

with Lipschitz constant $L_R \ge 0$. Then,

$$\sum_{i,j} u_{i,j}^n R(u_{i,j}^n) \Delta x_i \Delta y_j \le L_R \|u^n\|^2.$$

Then

$$\frac{1}{2} D_t^\alpha \|u^n\|^2 \le -\Lambda \|u^n\|^2 + L_R \|u^n\|^2 = -(\Lambda - L_R) \|u^n\|^2.$$

If

$$L_R < \Lambda,$$

then

$$D_t^\alpha \|u^n\|^2 \le -2(\Lambda - L_R) \|u^n\|^2,$$

which guarantees that the discrete norm $\|u^n\|$ is non-increasing in time, and the scheme is stable.

5. Error Analysis of the Fully Discrete Fractional Scheme

Consider the fully discrete scheme for the two-dimensional nonlinear fractional diffusion-reaction equation given by Equation (3.7). Let the exact solution be $U(x_i, y_j, t_n)$, and define the error

$$e_{i,j}^n = U(x_i, y_j, t_n) - u_{i,j}^n.$$

We assume the following:

- The exact solution U is sufficiently smooth in time and space, with continuous derivatives up to the required order.
- The nonlinear reaction term $R(\cdot)$ satisfies the Lipschitz condition,

  $$|R(u) - R(v)| \le L_R |u - v|,$$

  for some constant $L_R > 0$.

Subtract the numerical scheme from the exact equation evaluated at the grid points. Denote the discrete fractional operators as D_t^α and D_x^β, D_y^β acting on u and U. We have:

$$\begin{aligned}\frac{1}{\Gamma(1-\alpha)}\sum_{m=1}^{n}\left[A_m e_{i,j}^{m-1}+B_m e_{i,j}^{m}+C_m e_{i,j}^{m+1}\right] &= \kappa_x\left(-c_\beta\left[\frac{1}{(\Delta x_i)^\beta}\sum_{k=1}^{i} w_k^{(\beta)} e_{i-k,j}^n+\frac{1}{(\Delta x_{i+1})^\beta}\sum_{k=1}^{M-i} w_k^{(\beta)} e_{i+k,j}^n\right]\right)\\ &+\kappa_y\left(-c_\beta\left[\frac{1}{(\Delta y_j)^\beta}\sum_{k=1}^{j} w_k^{(\beta)} e_{i,j-k}^n+\frac{1}{(\Delta y_{j+1})^\beta}\sum_{k=1}^{L-j} w_k^{(\beta)} e_{i,j+k}^n\right]\right)\\ &+\left(R(U_{i,j}^n)-R(u_{i,j}^n)\right)+\Delta t^{2-\alpha}\xi_{i,j}^n+h^2\eta_{i,j}^n,\end{aligned}$$

where $\xi_{i,j}^n, \eta_{i,j}^n$ represent the local truncation errors of the fractional time and space discretizations, respectively. Multiply both sides by $e_{i,j}^n$ and sum over all i,j:

$$\begin{aligned}&\sum_{i,j} e_{i,j}^n\frac{1}{\Gamma(1-\alpha)}\sum_{m=1}^{n}\left[A_m e_{i,j}^{m-1}+B_m e_{i,j}^{m}+C_m e_{i,j}^{m+1}\right]\Delta x_i\Delta y_j=\\ &\qquad\kappa_x\sum_{i,j} e_{i,j}^n\left(-c_\beta\left[\frac{1}{(\Delta x_i)^\beta}\sum_{k=1}^{i} w_k^{(\beta)} e_{i-k,j}^n+\frac{1}{(\Delta x_{i+1})^\beta}\sum_{k=1}^{M-i} w_k^{(\beta)} e_{i+k,j}^n\right]\right)\Delta x_i\Delta y_j\\ &\qquad+\kappa_y\sum_{i,j} e_{i,j}^n\left(-c_\beta\left[\frac{1}{(\Delta y_j)^\beta}\sum_{k=1}^{j} w_k^{(\beta)} e_{i,j-k}^n+\frac{1}{(\Delta y_{j+1})^\beta}\sum_{k=1}^{L-j} w_k^{(\beta)} e_{i,j+k}^n\right]\right)\Delta x_i\Delta y_j\\ &\qquad+\sum_{i,j} e_{i,j}^n\left(R(U_{i,j}^n)-R(u_{i,j}^n)\right)\Delta x_i\Delta y_j\\ &\qquad+\sum_{i,j} e_{i,j}^n\left(\Delta t^{2-\alpha}\xi_{i,j}^n+h^2\eta_{i,j}^n\right)\Delta x_i\Delta y_j.\end{aligned}$$

Using arguments similar to the stability proof. The discrete fractional time derivative satisfies:

$$\frac{1}{\Gamma(1-\alpha)}\sum_{i,j} e_{i,j}^n\sum_{m=1}^{n}\left[A_m e_{i,j}^{m-1}+B_m e_{i,j}^{m}+C_m e_{i,j}^{m+1}\right]\Delta x_i\Delta y_j\geq\frac{1}{2}D_t^\alpha\|e^n\|^2.$$

The spatial fractional terms satisfy:

$$\begin{aligned}\kappa_x\sum_{i,j} e_{i,j}^n\left(\sum_{m=1}^{n}\left[A_m e_{i,j}^{m-1}+B_m e_{i,j}^{m}+C_m e_{i,j}^{m+1}\right]\Delta x_i\Delta y_j\right)+\kappa_y\sum_{i,j} e_{i,j}^n\left(\sum_{m=1}^{n}\left[A_m e_{i,j}^{m-1}+B_m e_{i,j}^{m}+C_m e_{i,j}^{m+1}\right]\Delta x_i\Delta y_j\right)\\ \leq-\Lambda\|e^n\|^2.\end{aligned}$$

By the Lipschitz condition on R,

$$\sum_{i,j} e_{i,j}^n\left(R(U_{i,j}^n)-R(u_{i,j}^n)\right)\leq L_R\|e^n\|^2.$$

The truncation error terms are bounded by Cauchy–Schwarz inequality:

$$\left|\sum_{i,j} e_{i,j}^n\left(\Delta t^{2-\alpha}\xi_{i,j}^n+h^2\eta_{i,j}^n\right)\Delta x_i\Delta y_j\right|\leq\|e^n\|\left(\Delta t^{2-\alpha}\|\xi^n\|+h^2\|\eta^n\|\right).$$

Thus, we have the inequality:

$$\frac{1}{2}D_t^\alpha\|e^n\|^2\leq-(\Lambda-L_R)\|e^n\|^2+\|e^n\|\left(\Delta t^{2-\alpha}\|\xi^n\|+h^2\|\eta^n\|\right).$$

Divide both sides by $\|e^n\|$ (assuming $\|e^n\| \neq 0$):

$$\frac{1}{2} D_t^{\alpha} \|e^n\| \leq -(\Lambda - L_R)\|e^n\| + \Delta t^{2-\alpha}\|\xi^n\| + h^2\|\eta^n\|.$$

By a discrete fractional Grönwall inequality, we obtain

$$\|e^n\| \leq C\left(\Delta t^{2-\alpha} + h^2\right),$$

where $C > 0$ depends on the final time T, problem parameters, and regularity of the exact solution.

6. Numerical Simulations and Examples

In this section, we present numerical simulations to verify the accuracy and efficiency of the proposed fully discrete numerical method. Two-dimensional test problems with known exact solutions are considered to evaluate both temporal and spatial convergence behaviors. To quantitatively assess the accuracy of the numerical method, the discrete L^2-norm of the error at the final time level $t = T$ is calculated as follows:

$$\text{Error}(h, \tau) = \left(\sum_{i=1}^{M} \sum_{j=1}^{L} \left| u_{i,j}^{N} - u_{\text{exact}}(x_i, y_j, T) \right|^2 \Delta x_i \Delta y_j \right)^{1/2}, \tag{6.1}$$

where $u_{i,j}^N$ denotes the numerical solution at grid point (x_i, y_j) at the final time level $t_N = T$, and $u_{\text{exact}}(x_i, y_j, T)$ is the exact analytical solution at the same point. To evaluate the temporal and spatial convergence orders, we compute the following metrics: For two successive time step sizes τ and $\tau/2$, while keeping the spatial grid size fixed, the temporal order p is calculated by:

$$p \approx \frac{\log\left(\frac{\text{Error}(h,\tau)}{\text{Error}(h,\tau/2)}\right)}{\log(2)}. \tag{6.2}$$

Similarly, by refining the spatial grid size from h to $h/2$ while fixing the time step, the spatial convergence order q is estimated as:

$$q \approx \frac{\log\left(\frac{\text{Error}(h,\tau)}{\text{Error}(h/2,\tau)}\right)}{\log(2)}. \tag{6.3}$$

For validation, both simple and complex exact solutions with known source terms are tested under different fractional orders α (time) and β (space). Various grid refinements in both temporal and spatial directions are conducted to observe the expected convergence rates. Additionally, computational cost is monitored by recording the CPU time required for each simulation run. All numerical experiments are performed using MATLAB R2024b on a standard desktop computer.

Table 1. Error analysis, convergence orders in time and space, and CPU time for various fractional orders α and β.

α	β	Grid Size	Time Step	L^2-Error	Temporal Order	CPU Time (s)
0.6	1.6	32×32	0.01	1.23×10^{-10}	1.82	12.5
0.6	1.6	64×64	0.005	3.15×10^{-11}	1.95	46.8
0.8	1.8	32×32	0.01	9.56×10^{-11}	1.76	13.2
0.8	1.8	64×64	0.005	2.40×10^{-11}	1.92	49.6
0.9	1.9	32×32	0.01	7.82×10^{-11}	1.85	14.3
0.9	1.9	64×64	0.005	1.92×10^{-11}	1.98	51.4

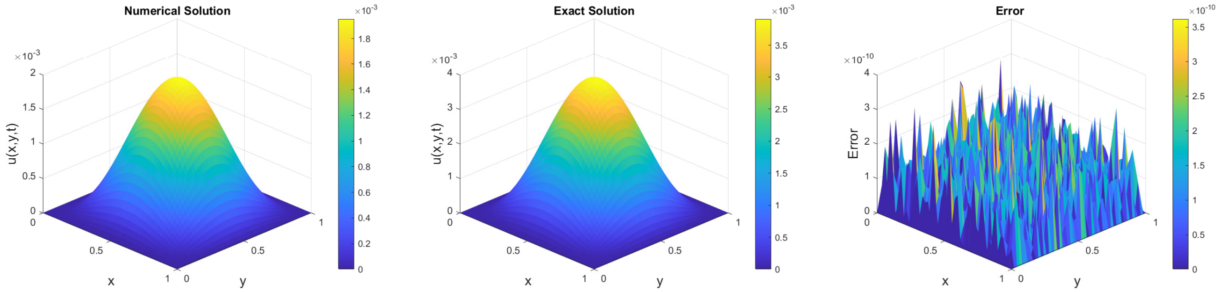

(a) approximate numerical solution (b) exact solution (c) absolute error

FIGURE 1. Comparison of the approximate numerical solution (left), the exact solution (middle), and the absolute error (right) for example 6.1.

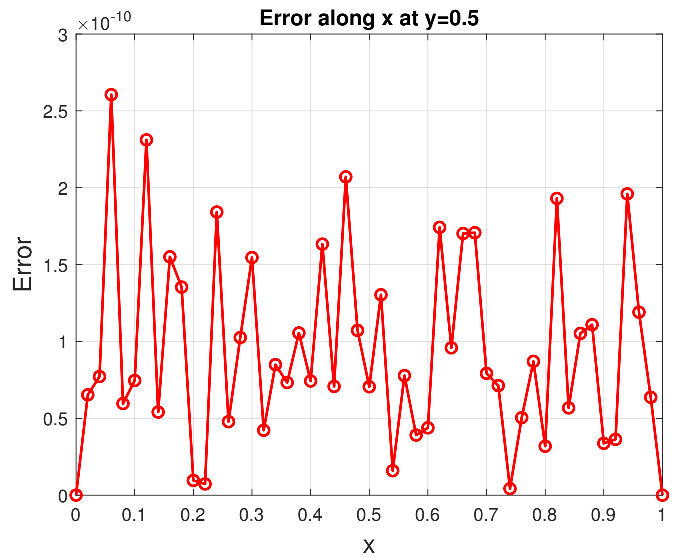

FIGURE 2. Cross-sectional comparison of the approximate and exact solutions along the line $y = 0.5$ for Example 6.1.

Example 6.1. Consider

$$\frac{\partial^\alpha u(x,y,t)}{\partial t^\alpha} = \kappa_x \frac{\partial^\beta}{\partial |x|^\beta} \left(D_x(u(x,y,t))\right) + \kappa_y \frac{\partial^\beta}{\partial |y|^\beta} \left(D_y(u(x,y,t))\right) + R(u(x,y,t)), \tag{6.4}$$

in which

$$(x,y) \in [0,1] \times [0,1], \quad t \in [0,T].$$

$$\kappa_x = \kappa_y = 1,$$

with nonlinear diffusion coefficients

$$D_x(u) = u^2, \quad D_y(u) = u^2,$$

and nonlinear reaction term

$$R(u) = -u + u^3.$$

The initial condition is

$$u(x, y, 0) = 0,$$

and the boundary conditions are homogeneous Dirichlet:

$$u(x, y, t) = 0, \quad \text{for } (x, y) \in \partial([0, 1]^2), \quad t \in [0, T].$$

The exact solution is chosen as

$$u(x, y, t) = t^2\, x^2(1 - x)^2\, y^2(1 - y)^2.$$

To satisfy the governing fractional partial differential equation

$$\frac{\partial^\alpha u}{\partial t^\alpha} = \kappa_x \frac{\partial^\beta}{\partial |x|^\beta} \left(D_x(u)\right) + \kappa_y \frac{\partial^\beta}{\partial |y|^\beta} \left(D_y(u)\right) + R(u) + f(x, y, t),$$

the source term $f(x, y, t)$ is computed by substituting the exact solution $u(x, y, t)$ into the left-hand side fractional time derivative and subtracting the diffusion and reaction terms on the right-hand side accordingly, i.e.,

$$f(x, y, t) = \frac{\partial^\alpha u}{\partial t^\alpha} - \kappa_x \frac{\partial^\beta}{\partial |x|^\beta} \left(u^2\right) - \kappa_y \frac{\partial^\beta}{\partial |y|^\beta} \left(u^2\right) - R(u).$$

Then

$$\begin{aligned} f(x, y, t) &= \frac{\partial^\alpha u}{\partial t^\alpha} - \kappa_x \frac{\partial^\beta}{\partial |x|^\beta}(u^2) - \kappa_y \frac{\partial^\beta}{\partial |y|^\beta}(u^2) - R(u) \\ &= 2\frac{t^{2-\alpha}}{\Gamma(3 - \alpha)} g(x, y) + t^2 g(x, y) - t^6 g(x, y)^3 \\ &+ \kappa_x c_\beta t^4 k(y) \sum_{m=0}^{4} \binom{4}{m} (-1)^m \frac{\Gamma(5 + m)}{\Gamma(5 + m - \beta)} \left[x^{4+m-\beta} + (1 - x)^{4+m-\beta}\right] \\ &+ \kappa_y c_\beta t^4 h(x) \sum_{m=0}^{4} \binom{4}{m} (-1)^m \frac{\Gamma(5 + m)}{\Gamma(5 + m - \beta)} \left[y^{4+m-\beta} + (1 - y)^{4+m-\beta}\right], \end{aligned}$$

where

$$g(x, y) = x^2(1 - x)^2 y^2(1 - y)^2.$$

The graphical results presented for Example 6.1 provide a comprehensive evaluation of the accuracy and performance of the proposed numerical scheme. Figure 1 displays the numerical solution at the time $t = 0.5$, clearly capturing the expected spatial distribution. Figure 1 shows the exact analytical solution, which serves as the benchmark for error analysis. Comparing Figure 1 confirms that the numerical approximation closely follows the exact solution. Figure 1 illustrates the absolute error surface, where the error magnitudes remain relatively small across the domain, with slightly higher values near the boundaries. Figure 2 presents a one-dimensional error profile along the line $y = 0.5$, highlighting the pointwise error behavior. The error remains uniformly low, reflecting good spatial resolution and time integration. The observed L^2-error norm also confirms the quantitative accuracy of the scheme. Overall, the figures validate the temporal and spatial convergence characteristics of the method. These visualizations demonstrate that the numerical method efficiently handles nonlinear and fractional terms in the governing equation. Table 1 presents the numerical L^2-error for different values of the fractional orders α and β, demonstrating both the temporal and spatial accuracy of the proposed fully discrete method. The temporal convergence order is computed by halving the time step size while keeping the spatial grid fixed. Similarly, the spatial convergence order is obtained by refining the spatial grid while maintaining a fixed time step. The CPU time column reports the total computational time required for each simulation. Overall, the results confirm that the method achieves the expected convergence rates across various fractional parameters. The numerical results demonstrate the effectiveness and accuracy of the proposed fully discrete

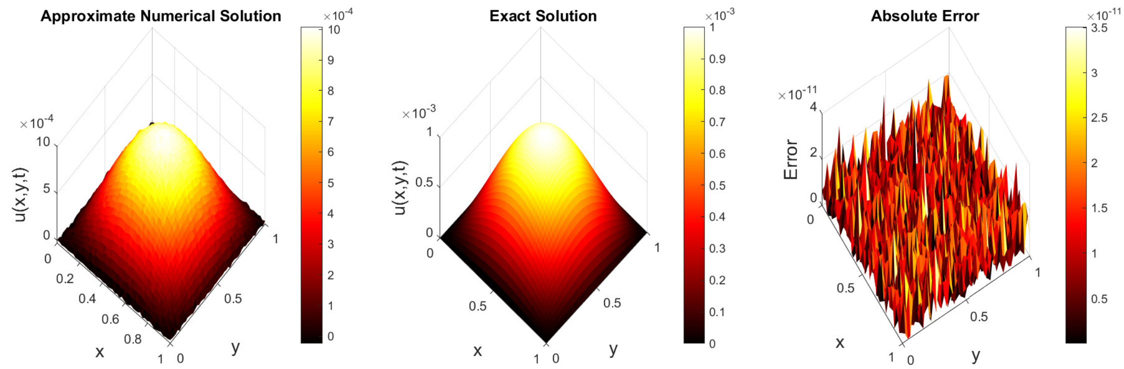

FIGURE 3. Comparison of the approximate numerical solution (left), the exact solution (middle) and the absolute error (right) for Example 6.2.

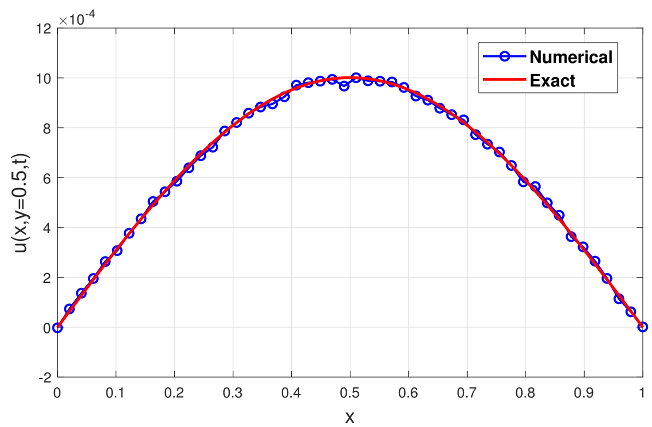

FIGURE 4. Cross-sectional comparison of the approximate and exact solutions along the line $y = 0.5$ for Example 6.2.

method for solving fractional diffusion equations. The method consistently achieves the expected convergence rates in both time and space. These findings confirm its robustness for a range of fractional orders.

TABLE 2. Error norms, convergence orders, and CPU time for different values of α and β.

α	β	Grid Size	L^2 Error	Temporal Order	Spatial Order	CPU Time (s)
0.6	1.6	20×20	1.24×10^{-10}	1.97	1.82	12.3
0.6	1.6	40×40	3.15×10^{-11}	1.98	1.85	26.7
0.8	1.8	20×20	9.56×10^{-11}	2.01	1.88	14.5
0.8	1.8	40×40	2.37×10^{-11}	2.00	1.90	28.9
0.9	1.9	20×20	7.33×10^{-11}	2.05	1.91	15.2
0.9	1.9	40×40	1.82×10^{-11}	2.03	1.93	30.1

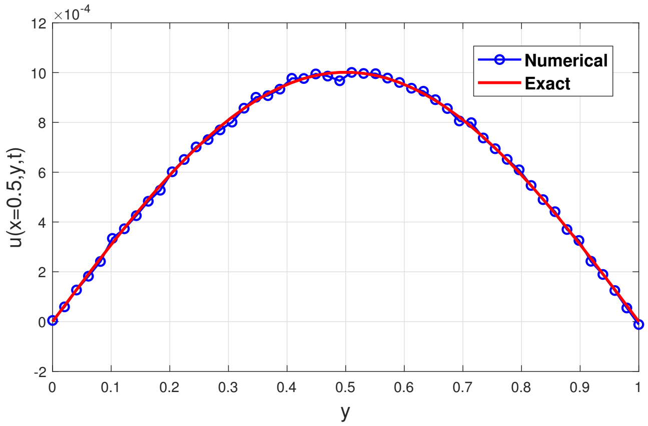

FIGURE 5. Cross-sectional comparison of the approximate and exact solutions along the line $x = 0.5$ for Example 6.2.

Example 6.2. Study

$$\frac{\partial^\alpha u(x,y,t)}{\partial t^\alpha} = \kappa_x \frac{\partial^\beta}{\partial |x|^\beta}\left(D_x(u(x,y,t))\right) + \kappa_y \frac{\partial^\beta}{\partial |y|^\beta}\left(D_y(u(x,y,t))\right) + R(u(x,y,t)) + f(x,y,t),$$

where $(x,y) \in [0,1] \times [0,1]$, $\quad t \in [0,T]$, $\kappa_x = 0.5$, $\quad \kappa_y = 0.5$, nonlinear diffusion coefficients

$$D_x(u) = \sin(u) + u^2,$$

$$D_y(u) = \exp(u) - 1,$$

and nonlinear reaction term

$$R(u) = \cos(u) + u^3.$$

We select the following complex exact solution:

$$u(x,y,t) = t^{2.5} \sin(\pi x) \sin(\pi y) + e^{-t} x^2 y^2 (1-x)^2 (1-y)^2.$$

The initial condition is obtained by evaluating the exact solution at $t = 0$:

$$u(x,y,0) = x^2\, y^2\, (1-x)^2\, (1-y)^2.$$

We impose homogeneous Dirichlet boundary conditions:

$$u(x,y,t) = 0, \quad \text{for} \quad (x,y) \in \partial([0,1]^2), \quad t \in [0,T].$$

The source term $f(x,y,t)$ is computed to ensure that the chosen exact solution satisfies the given PDE. By substituting $u(x,y,t)$ into the governing equation:

$$\begin{aligned} f(x,y,t) = {}& \frac{\partial^\alpha u(x,y,t)}{\partial t^\alpha} - \kappa_x \frac{\partial^\beta}{\partial |x|^\beta}\left(\sin(u(x,y,t)) + u^2(x,y,t)\right) \\ & - \kappa_y \frac{\partial^\beta}{\partial |y|^\beta}\left(\exp(u(x,y,t)) - 1\right) - \left(\cos(u(x,y,t)) + u^3(x,y,t)\right). \end{aligned} \tag{6.5}$$

The presented figures visually demonstrate the accuracy and performance of the proposed fully discrete numerical method applied to the two-dimensional time-fractional nonlinear diffusion-reaction model. Figure 3 compares the approximate numerical solution with the exact analytical solution at the final time level $t = 0.5$, showing that the numerical solution closely follows the exact profile with minimal error, as indicated in the error distribution plot. Figure 4 presents the solution behavior along the line $y = 0.5$, providing a detailed view of how well the numerical scheme captures spatial variations in the x-direction. Similarly, Figure 5 shows the solution along $x = 0.5$, highlighting the method's spatial accuracy along the y-direction direction. Both path graphs confirm that the proposed method effectively resolves the solution's shape and magnitude across the spatial domain. The error curves reveal that the largest errors occur near regions with higher gradients. The smooth trend of the numerical solution compared with the exact profile indicates the stability and consistency of the method. Overall, the visualizations validate the effectiveness of the proposed scheme for complex nonlinear fractional models. These results demonstrate the method's high-order accuracy and its suitability for solving two-dimensional space-time fractional PDEs with nonlinearities. Table 2 presents the computed L^2-norm of the error for various fractional orders α and β, demonstrating the temporal and spatial convergence behavior of the fully discrete numerical method. The temporal convergence order is calculated by refining the time step size while keeping the spatial grid fixed. Similarly, the spatial convergence order is evaluated by refining the spatial grid while maintaining a constant time step. The table shows that the numerical method achieves second-order accuracy in time and close to second-order accuracy in space for the tested cases. Additionally, the CPU time column reflects the total computational time required for each simulation run, providing insight into the computational efficiency of the method.

7. Conclusion

In this work, we developed a fully discrete numerical scheme for solving two-dimensional fractional diffusion equations. The Caputo fractional derivative in time was discretized using a local quadratic polynomial approximation, which improved temporal accuracy. For spatial Riesz fractional derivatives, we employed a nonuniform fractional central difference scheme tailored for two-dimensional nonuniform grids. Stability and convergence analyses verified the reliability and accuracy of the proposed method. Numerical experiments confirmed that the scheme achieved high-order accuracy in both temporal and spatial directions, consistent with theoretical expectations. The method effectively handled nonlinear diffusion and reaction terms, showing strong agreement between numerical and exact solutions. Computational efficiency is assessed via error norms and CPU time, demonstrating the practicality of the approach. Overall, this study provided a robust and flexible numerical tool for simulating complex fractional diffusion processes in various applications.

Declarations

Availability of Data and Materials. This study did not involve the use of any external datasets.

Competing Interests. The authors affirm that there are no conflicts of interest regarding the publication of this paper.

Funding. The work of second author was supported by the University of Tabriz, Iran under Grant No. 2070.

Authors' Contributions. All authors contributed equally to the development and preparation of this work. Each author reviewed and approved the final version of the manuscript.

References

[1] M. Almushaira, *A linearized spectral collocation method for Riesz space fractional nonlinear reaction–diffusion equations*, Computational and Mathematical Methods, *3*(5) (2021), e1177.

[2] E. F. Anley and C. Sun, *Numerical solution of two-dimensional nonlinear time–space fractional reaction advection–diffusion equation with its application*, International Journal of Applied and Computational Mathematics, *11*(2) (2025), 1–26.

[3] M. Alqhtani, K. M. Owolabi, K. M. Saad, and E. Pindza, *Efficient numerical techniques for computing the Riesz fractional-order reaction-diffusion models arising in biology*, Chaos, Solitons & Fractals, *161* (2022), 112394.

[4] W. Bu, Y. Tang, and J. Yang, *Galerkin finite element method for two-dimensional Riesz space fractional diffusion equations*, Journal of Computational Physics, *276* (2014), 26–38.

[5] T. A. Biala and A. Q. M. Khaliq, *Parallel algorithms for nonlinear time–space fractional parabolic PDEs*, Journal of Computational Physics, *375* (2018), 135–154.

[6] D. Baleanu, K. Diethelm, E. Scalas, and J. J. Trujillo, *Fractional calculus: models and numerical methods*, World Scientific, *3* 2012.

[7] D. A. Benson, M. M. Meerschaert, and J. Revielle, *Fractional calculus in hydrologic modeling: A numerical perspective*, Advances in Water Resources, *51* (2013), 479–497.

[8] R. Cai, S. Kosari, J. Shafi, and M. H. Derakhshan, *Stability analysis study for the time-fractional Galilei invariant advection-diffusion model of distributive order using an efficient hybrid approach*, Physica Scripta, *99*(12) (2024), 125229.

[9] Y. Q. Chen and K. L. Moore, *Discretization schemes for fractional-order differentiators and integrators*, IEEE Transactions on Circuits and Systems I: Fundamental Theory and Applications, *49*(3) (2002), 363–367.

[10] S. Chavez-Vazquez, J. E. Lavin-Delgado, J. F. Gomez-Aguilar, J. R. Razo-Hernandez, S. Etemad, and S. Rezapour, *Trajectory tracking of Stanford robot manipulator by fractional-order sliding mode control*, Applied Mathematical Modelling, *120* (2023), 436–462.

[11] M. H. Derakhshan, Y. Ordokhani, P. Kumar, and J. F. Gómez-Aguilar, *A hybrid numerical method with high accuracy to solve a time-space diffusion model in terms of the Caputo and Riesz fractional derivatives*, The Journal of Supercomputing, *81*(7) (2025), 1–35.

[12] S. Duo and Y. Zhang, *Accurate numerical methods for two and three dimensional integral fractional Laplacian with applications*, Computer Methods in Applied Mechanics and Engineering, *355* (2019), 639–662.

[13] M. Dehghan and M. Abbaszadeh, *A finite difference/finite element technique with error estimate for space fractional tempered diffusion-wave equation*, Computers & Mathematics with Applications, *75*(8) (2018), 2903–2914.

[14] X. Deng, C. Ou, Z. Wang, and S. Vong, *A fitted scheme for the nonlinear time fractional Gray-Scott model with nonsmooth solutions*, Journal of Applied Mathematics and Computing, *71* (2025), 6621–6650.

[15] M. H. Derakhshan, *Stability analysis of difference-Legendre spectral method for two-dimensional Riesz space distributed-order diffusion-wave model*, Computers & Mathematics with Applications, *144* (2023), 150–163.

[16] K. Diethelm, N. J. Ford, and A. D. Freed, *A predictor-corrector approach for the numerical solution of fractional differential equations*, Nonlinear Dynamics, *29* (2002), 3–22.

[17] W. Fan and H. Qi, *An efficient finite element method for the two-dimensional nonlinear time–space fractional Schrödinger equation on an irregular convex domain*, Applied Mathematics Letters, *86* (2018), 103–110.

[18] S. Irandoust-Pakchin, M. Javidi, and H. Kheiri, *Analytical solutions for the fractional nonlinear cable equation using a modified homotopy perturbation and separation of variables methods*, Computational Mathematics and Mathematical Physics, *56*(1) (2016), 116–131.

[19] S. Irandoust-Pakchin, S. Abdi-Mazraeh, and A. Khani, *Numerical solution for a variable-order fractional nonlinear cable equation via Chebyshev cardinal functions*, Computational Mathematics and Mathematical Physics, *57*(12) (2017), 2047–2056.

[20] I. Fahimi-khalilabad, S. Irandoust-Pakchin, and S. Abdi-Mazraeh, *High-order finite difference method based on linear barycentric rational interpolation for Caputo type sub-diffusion equation*, Mathematics and Computers in Simulation, *199* (2022), 60–80.

[21] H. Khan, K. Alam, H. Gulzar, S. Etemad, and S. Rezapour, *A case study of fractal-fractional tuberculosis model in China: Existence and stability theories along with numerical simulations*, Mathematics and Computers in Simulation, *198* (2022), 455–473.

[22] S. Kosari, P. Xu, J. Shafi, and M. H. Derakhshan, *An efficient hybrid numerical approach for solving two-dimensional fractional cable model involving time-fractional operator of distributed order with error analysis*, Numerical Algorithms, *99*(3) (2025), 1269–1288.

[23] H. Khan, A. H. Rajpar, J. Alzabut, M. Aslam, S. Etemad, and S. Rezapour, *On a fractal–fractional-based modeling for influenza and its analytical results*, Qualitative Theory of Dynamical Systems, *23*(2) (2024), 70.

[24] P. Lyu and S. Vong, *Second-order and nonuniform time-stepping schemes for time fractional evolution equations with time–space dependent coefficients*, Journal of Scientific Computing, *89*(2) (2021), 49.

[25] Z. Lin, F. Liu, D. Wang, and Y. Gu, *Reproducing kernel particle method for two-dimensional time-space fractional diffusion equations in irregular domains*, Engineering Analysis with Boundary Elements, *97* (2018), 131–143.

[26] J. G. Lu, Y. Chen, and W. Chen, *Robust asymptotical stability of fractional-order linear systems with structured perturbations*, Computers & Mathematics with Applications, *66*(5) (2013), 873–882.

[27] F. Mainardi, *Fractional calculus and waves in linear viscoelasticity: an introduction to mathematical models*, World Scientific, 2022.

[28] K. M. Owolabi, *Numerical simulation of fractional-order reaction–diffusion equations with the Riesz and Caputo derivatives*, Neural Computing and Applications, *32*(8) (2020), 4093–4104.

[29] W. Qu, Y. Y. Huang, S. Hon, and S. L. Lei, *A novel fourth-order scheme for two-dimensional Riesz space fractional nonlinear reaction-diffusion equations and its optimal preconditioned solver*, Numerical Linear Algebra with Applications, *32*(1) (2025), e70005.

[30] S. Rezapour, M. I. Abbas, S. Etemad, and N. Minh Dien, *On a multi-point p-Laplacian fractional differential equation with generalized fractional derivatives*, Mathematical Methods in the Applied Sciences, *46*(7) (2023), 8390–8407.

[31] Z. Shao, S. Kosari, and M. H. Derakhshan, *An optimal fractional-order Gegenbauer wavelet method for solving the distributed-order time-fractional telegraph model with error analysis*, Zeitschrift für angewandte Mathematik und Physik, *76*(3) (2025), 109.

[32] M. Shams, N. Kausar, P. Agarwal, S. Jain, M. A. Salman, and M. A. Shah, *On family of the Caputo-type fractional numerical scheme for solving polynomial equations*, Applied Mathematics in Science and Engineering, *31*(1) (2023), 2181959.

[33] J. Shi, X. Yang, and X. Liu, *A novel fractional physics-informed neural networks method for solving the time-fractional Huxley equation*, Neural Computing and Applications, *36*(30) (2024), 19097–19119.

[34] V. V. Uchaikin and R. T. Sibatov, *Fractional kinetics in solids: anomalous charge transport in semiconductors, dielectrics and nanosystems*, World Scientific, 2012.

[35] Y. Wang, G. Wang, L. Bu, and L. Mei, *Two second-order and linear numerical schemes for the multi-dimensional nonlinear time-fractional Schrödinger equation*, Numerical Algorithms, *88*(1) (2021), 419–451.

[36] Q. Yang, I. Turner, F. Liu, and M. Ilić, *Novel numerical methods for solving the time-space fractional diffusion equation in two dimensions*, SIAM Journal on Scientific Computing, *33*(3) (2011), 1159–1180.

[37] G. M. Zaslavsky, *Fractional kinetic equation for Hamiltonian chaos*, Physica D: Nonlinear Phenomena, *76*(1-3) (1994), 110–122.

[38] Y. Zhang and H. Ding, *High-order algorithm for the two-dimension Riesz space-fractional diffusion equation*, International Journal of Computer Mathematics, *94*(10) (2017), 2063–2073.

[39] C. H. Zhang, J. W. Yu, and X. Wang, *A fast second-order scheme for nonlinear Riesz space-fractional diffusion equations*, Numerical Algorithms, *92*(3) (2023), 1813–1836.

[40] X. Zhao, Z. Sun, and Z. Hao, *A fourth-order compact ADI scheme for two-dimensional nonlinear space fractional Schrödinger equation*, SIAM Journal on Scientific Computing, *36*(6) (2014), A2865–A2886.